Journal of Electrochemistry

Volume 28 | Issue 1

2022-01-28

A Flexible Enzymeless Glucose Sensor via Electrodepositing 3D Flower-like CoS onto Self-Supporting Graphene Tape Electrode

Jiang Li

Zuo-Peng Li

Yun-Feng Bai

Su-Xing Luo

Yong Guo

Ya-Yan Bao

Rong Li

See next page for additional authors

Recommended Citation

Jiang Li, Zuo-Peng Li, Yun-Feng Bai, Su-Xing Luo, Yong Guo, Ya-Yan Bao, Rong Li, Hai-Yan Liu, Feng Feng. A Flexible Enzymeless Glucose Sensor via Electrodepositing 3D Flower-like CoS onto Self-Supporting Graphene Tape Electrode[J]. *Journal of Electrochemistry*, 2022 , 28(1): 2104211.
DOI: 10.13208/j.electrochem.210421
Available at: https://jelectrochem.xmu.edu.cn/journal/vol28/iss1/4

A Flexible Enzymeless Glucose Sensor via Electrodepositing 3D Flower-like CoS onto Self-Supporting Graphene Tape Electrode

Authors

Jiang Li, Zuo-Peng Li, Yun-Feng Bai, Su-Xing Luo, Yong Guo, Ya-Yan Bao, Rong Li, Hai-Yan Liu, and Feng Feng

Corresponding Author(s)

Feng Feng(feng-feng64@263.net)

【Article】 **DOI**: 10.13208/j.electrochem.210421 **Http**://electrochem.xmu.edu.cn

A Flexible Enzymeless Glucose Sensor via Electrodepositing 3D Flower-like CoS onto Self-Supporting Graphene Tape Electrode

Jiang Li[1], Zuo-Peng Li[1], Yun-Feng Bai[1], Su-Xing Luo[2], Yong Guo[1], Ya-Yan Bao[1], Rong Li[3], Hai-Yan Liu[4], Feng Feng[1*]

(*1. School of Chemistry and Chemical Engineering, Shanxi Datong University, Datong 037009, Shanxi, P.R. China; 2. Department of Chemistry and Chemical Engineering, Zunyi Normal College, Zunyi 563006, Guizhou, P.R. China; 3. College of Chemistry and Chemical Engineering, China West Normal University, Nanchong 637000, Sichuan, P.R. China; 4. School of Life and Science, Shanxi Datong University, Datong 037009, Shanxi, P.R. China*)

Abstract: Three-dimensional (3D) nanostructural Flower-like cobalt sulfide (CoS) on flexible self-supporting graphene tape electrode (GTE) with remarkably electrocatalytic activity toward glucose was successfully prepared by electrodeposition. Structural characterizations revealed that the electrodeposited CoS was highly dispersed on GTE as an active material. The fabricated binder-free and self-standing CoS/GTE shows a good linear response in the range of 0.025 ~ 1.0 mmol·L^{-1}, reaching a high glucose sensitivity value of 323.3 μA·(mmol·L^{-1})$^{-1}$·cm^{-2} and a low detection limit of 8.5 μmol·L^{-1} (S/N = 3). Moreover, the as-prepared sensor was well applied for glucose determination in human serum. Thus, the self-supporting, binder-free, low-cost sensor has good potential as a promising device for practical quantitative analysis of glucose in human serum.

Key words: flexible electrode; flower-like CoS; electrodeposition; glucose sensor

1 Introduction

It is of much significance to develop a fast and dependable method for glucose sensing due to its extensive application in many fields, including clinical diagnostics, biotechnology, and food industry[1-3]. As of now, lots of methodologies and processes have been applied for determining glucose, such as electrochemical methods[4], optical methods[5], colorimetry[6] and fluorescent spectroscopy[7]. Among the above-mentioned techniques, the electrochemical method has been becoming the most highly enticing for sensor research. According to the usage of the enzyme, the electrochemical glucose sensors could be separated into two types, the enzymatic and non-enzymatic sensors[4,8]. Glucose oxidase is a type of bio-enzyme with high sensitivity and selectivity to glucose, and has been widely utilized to develop various amperometric biosensors for detecting glucose, but the activity of enzyme could be disturbed by many factors such as humidity, toxic chemicals, temperature, pH, and the immobilized technology[9]. Many attempts have been made for direct detection of glucose by non-enzymatic sensors. Noble metals[10-14] own high catalytic activity for enzymeless glucose electrooxidation with their metal alloys[15-17], but it narrows their widespread applications due to the high cost of such catalysts. To solve these problems, it is highly desirable to exploit earth-ample nanomaterials for electrocatalytic glu-

Cite as: Li J, Li Z P, Bai Y F, Luo S X, Guo Y, Bao Y Y, Li R, Liu H Y, Feng F. A flexible enzymeless glucose sensor via electrodepositing 3D flower-like CoS onto self-supporting graphene tape electrode. *J. Electrochem.*, 2021, 28(1): 2104211.

Received: 2021-04-21, Revised: 2021-06-30. * Corresponding author, Tel: (86-352)7158662, E-mail: feng-feng64@263.net

cose sensing application.

Cobalt sulfides are striking transition metal chalcogenide owning to their catalytic activity, magnetic properties and potential as an up-and-coming electrode material of low cost and nanostructural cobalt chalcogenides have been extensively investigated as important electrocatalysts for splitting water and supercapacitors[18-19]. Recently, cobalt sulfides have come into being in the region of electrochemical analysis. Wu et al. reported a non-enzymatic glucose sensor (NEGS) by the use of tremella-like CoS with the sensitivity values of 139.35 μA·(mmol·L^{-1})$^{-1}$·cm^{-2} and 28.44 μA·(mmol·L^{-1})$^{-1}$·cm^{-2}, respectively[20]. In addition, Qu et al. reported the CoS-decorated 3D porous carbon skeleton on glassy carbon electrode (GCE) for NEGS with a linear detection range of 0.010 mmol·L^{-1} to 0.960 mmol·L^{-1} and a low limit of detection (LOD) of 2 μmol·L^{-1}[21]. Meng and coworkers prepared Co_xS_y/rGO-PEDOT/GCE by cyclic voltammetry (CV) used for glucose sensing with the sensitivity of 113.46 μA·(mmol·L^{-1})$^{-1}$·cm^{-2}[22]. Furthermore, Sivakumar et al. also fabricated cobalt sulfide nanorods for vanillin detection in food samples with a linear range from 0.5 to 56 μmol·L^{-1} and a LOD of 0.07 μmol·L^{-1}[23]. However, their synthesis was embroiled in convoluted preparation processes, long time, high temperature and require tiresome control of the reaction conditions. Furthermore, it is not convenient to use GCE due to its polishing before each use and narrow range of application.

In recent years, 3D graphene materials have been extensively researched in the forms of foams[24], sponges[25], aerogels[26], and hydrogels[27] with dominated porous structures because of their wide scope of potential applications, in energy conversion and storage, biology, catalysis, and environmental remediation[28-30]. However, it remains to be a dispiriting challenge and impeded by the intricate and time-consuming procedures for the synthesis of 3D graphene materials. Recently, a 3D porous graphene tape electrode (GTE) as a self-supporting matrix was proposed, which showed good electron transfer ability with a broad potential window (2.0 V)[31]. Herein, Combining the advantages of GTE and cobalt sulfide nanomaterials, a facile flower-like CoS-based GTE biosensor design by direct electrodeposition was demonstrated for sensitive glucose detection for the first time. The obtained flower-like CoS showed an outstanding electrochemical performance for glucose detection.

2 Experimental

2.1 Reagents and Materials

Scotch transparent tape and commercial graphite foil were purchased from 3M Company and North China Technology Metal Material Company, respectively. Glucose, $CoSO_4·7H_2O$, KSCN, fructose, uric acid (UA), dopamine (DA), ascorbic acid (AA) and other reagents were purchased from Aladdin Ltd. Teflon tape and human blood serum samples were obtained from Chukoh Chemical Industries, Ltd., and Sangon Biotech Co., Ltd. (Shanghai, China). All chemicals were used without further purification unless otherwise indicated. Deionized-water was used throughout the study. Water was deionized with the Millipore Milli-Q UF Plus system.

2.2 Apparatus and Measurements

Scanning electron microscopy and energy dispersive X-ray spectrometry (SEM/EDS) employed in surface morphologic and elemental characterizations by field-emission scanning electron microscopy (SEM, FEI Quanta 650 FEG) at an accelerating voltage of 20 kV. X-ray photoelectron spectroscopic (XPS) measurements were performed by ESCALAB 250Xi X-ray photoelectron spectrometer.

The electrochemical tests were conducted by the use of a CHI660E electrochemical workstation (CH Instruments Inc., China) including a typical three-electrode cell equipped with the as-prepared CoS/GTE as the working electrode, Ag/AgCl (saturated KCl) electrode and Pt sheet as the reference and auxiliary electrodes, respectively. All the electrochemical tests were carried out in 0.1 mol·L^{-1} NaOH solution.

2.3 Preparation of the Flexible GTE

A simple peeling method was used for fabricating the GTEs following the previously reported one after slight modification[31]. Firstly, the commercial graphite foils were cut into proper size (2 cm × 5 cm), and then

they were polished using abrasive paper (grit 2000 and 5000). Secondly, after respective ultrasonic washing by acetone, ethanol, and ultrapure water for 15 min, the as-pretreated graphite foils were put into a drying oven at 60 °C for 12 h. Thirdly, an above-pretreated graphite foil was put onto a cleaning glass slab, and then the scotch transparent tape was manually applied and stuck to the piece of top surface of graphite foil. After pressed by a glass slide, the tape was quickly stripped off. Finally, the parts of the tape without graphite were sheared off to obtain the 3D porous self-standing flexible GTE. The area of GTEs exposed to the electrolyte solution was controlled by Teflon tape sealing and limited at 0.25 cm^2.

2.4 Electrodeposition of CoS on GTE

The cobalt sulfide (CoS) was electrochemically synthesized with cobalt sulfate ($CoSO_4$) as cobalt source and potassium thiocyanate (KSCN) as sulfur source. It is reported that SCN^- can bring in varieties of complexes with the assistance of S or N atom coordination with transition metal ions, and is also known to facilitate the electrochemical reactions using its two coordination sites with transition metal ions for adsorption onto an electrode surface[32, 33]. To prepare the CoS/GTE sensor, the pliable GTE set by electrode holder was submerged in an aqueous solution including 0.05 mol·L^{-1} $CoSO_4$, 0.2 mol·L^{-1} KSCN, and then, a potential of -1.0 V (vs. Ag/AgCl) was applied to the GTE via chronoamperometry technique for 20 min to electrodeposit CoS, whose electrochemical active area was calculated to be 6.69 cm^2 using the double layer capacitance in 1 mol·L^{-1} NaOH. The as-prepared sensor was washed with copious deionized water and dried at room temperature. The preparation procedure of CoS/GTE is depicted in Scheme 1.

3 Results and Discussion

3.1 Morphological Analysis

The structure and morphology of the as-prepared GTE were investigated by means of SEM. As displayed in Figure 1(A), the surface of GTE exhibited the typical folded and crumpled layered structure of graphene sheets with some exposed graphene edge planes on its surface, which denotes that the GTE could improve the electron transmission rate and multidimensional electron transfer pathways for the electrolyte solution. Figure 1(B) presents SEM image of CoS. It is interesting that 3D flower-like structure of CoS can be clearly seen, which is piled up from randomly interwoven nanosheets with the dimensions of several nanometers. It makes the surface area of CoS bigger due to the 3D hierarchical structure, bringing high catalytic activity. And it confirms the homogenous distribution of Co and S atoms in the plane of CoS (Figure 1(C) and (D)) by performing elemental mapping.

3.2 XPS Studies

XPS measurements were performed to further study

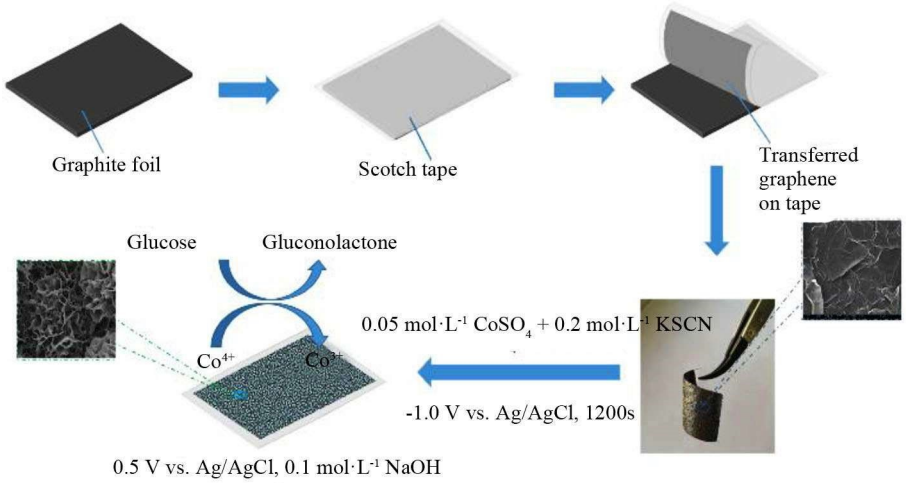

Scheme 1 Schematic illustration showing the synthetic process of CoS/GTE and the mechanism for glucose oxidation (color on line)

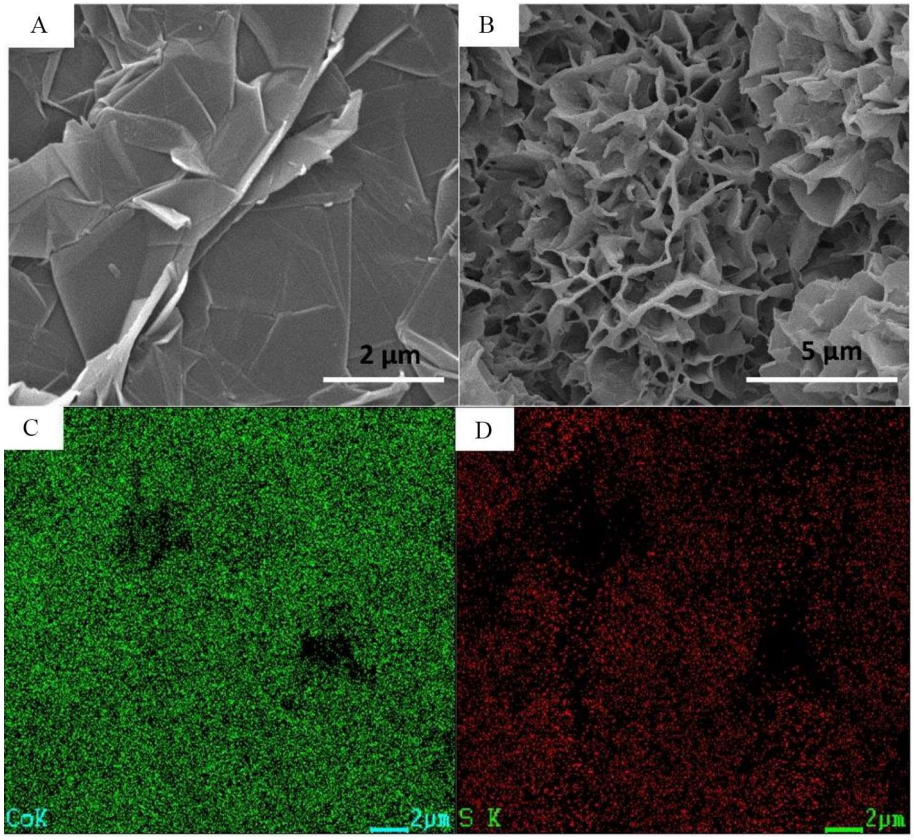

Figure 1 SEM images of (A) GTE and (B) CoS. EDX elemental mapping images of (C) Co and (D) S for CoS/GTE. (color on line)

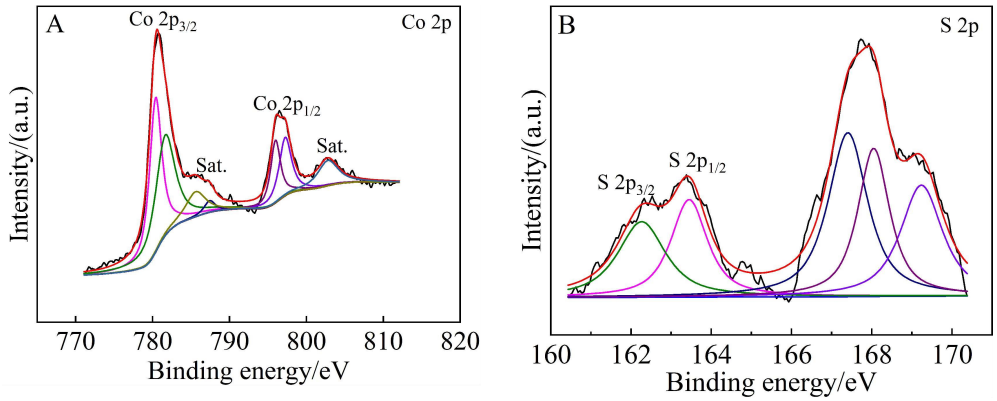

Figure 2 XPS spectra of Co 2p (A) and S 2p (B) of the electrodeposited CoS. (color on line)

the as-electrodeposited CoS. In Figure 2(A), the Co 2p spectrum displays a main characteristic peak at 780.78 eV with a shoulder peak at 796.49 eV, which is characteristic peak of Co^{2+} [34]. Another two peaks at 786.4 and 802.49 eV can be sequentially ascribed to the satellite peaks of Co $2p_{3/2}$ and Co $2p_{1/2}$. In S 2p region displayed in Figure 2(B), the two peaks at 163.36 eV and 162.3 eV correspond to the S $2p_{1/2}$ and S $2p_{3/2}$, separately, which relies on the existing sulfur ion on the surface and the Co-S bonds[35]. Specifically, the appearance of the additional peaks at ca. 164.5 ~ 168.6 eV should be attributed to the trivial amount of CoS byproducts since the electrodeposited CoS is generally a non-stoichiometric compound[36]. Another peak at 169.1 eV can be allotted to SO_4^{2-}, potentially resulting from the surface adsorbed $CoSO_4$[33, 37]. The

XPS results were in good agreement with the previous reported[38].

3.3 Electrochemical Behavior of Prepared CoS/GTE

Initially, the electrochemical performance of the as-prepared CoS/GTE was investigated in 0.1 mol·L^{-1} NaOH electrolyte via CV with a potential range from 0 to 0.7 V (vs. Ag/AgCl) at a scan rate of 50 mV·s^{-1}. As shown in Figure 3(A), no significant redox peaks were observed for GTE in the absence of glucose, which indicates that it is not electrochemically active in the potential window. In stark contrast, two pairs of redox peaks appeared andcorresponded to the reduction and oxidation processes of electrodeposited CoS on GTE's surface, which could be allotted to the Co^{2+}/Co^{3+} (labelled as I/II) and Co^{3+}/Co^{4+} (labelled as III/IV) redox couples.

Figure 3(B) shows the CVs of the CoS/GTE at different scan rates. The anodic peak moved a little positively, while the cathodic peak a negative shift with the increasing scan rate, denoting an electrochemically quasi-reversible electron transfer reaction for the reactions in equation (1) and (2)[39, 40]. In addition, as shown in Figure 3(C), both the oxidative and reductive peak currents varied linearly in proportion to the square root of scan rate, indicating that the redox reaction of CoS at the GTE surface is diffusion-regulated electrochemical process.

$$CoO + OH^- \rightleftharpoons CoOOH + H_2O + e^- \quad (1)$$

$$CoOOH + OH^- \rightleftharpoons CoO_2 + H_2O + e^- \quad (2)$$

Figure 3(D) shows the CVs of the CoS/GTE collected in different concentrations of glucose (0 ~ 1 mmol·L^{-1}) in 0.1 mol·L^{-1} NaOH solution at a scan rate of 50 mV·s^{-1}. A striking increase of anodic peak current was observed. It is indicative of the good electrocatalytic activity of CoS/GTE against the catalytic oxidation of glucose due to the increase of the anodic peak currents, implying that the CoS could

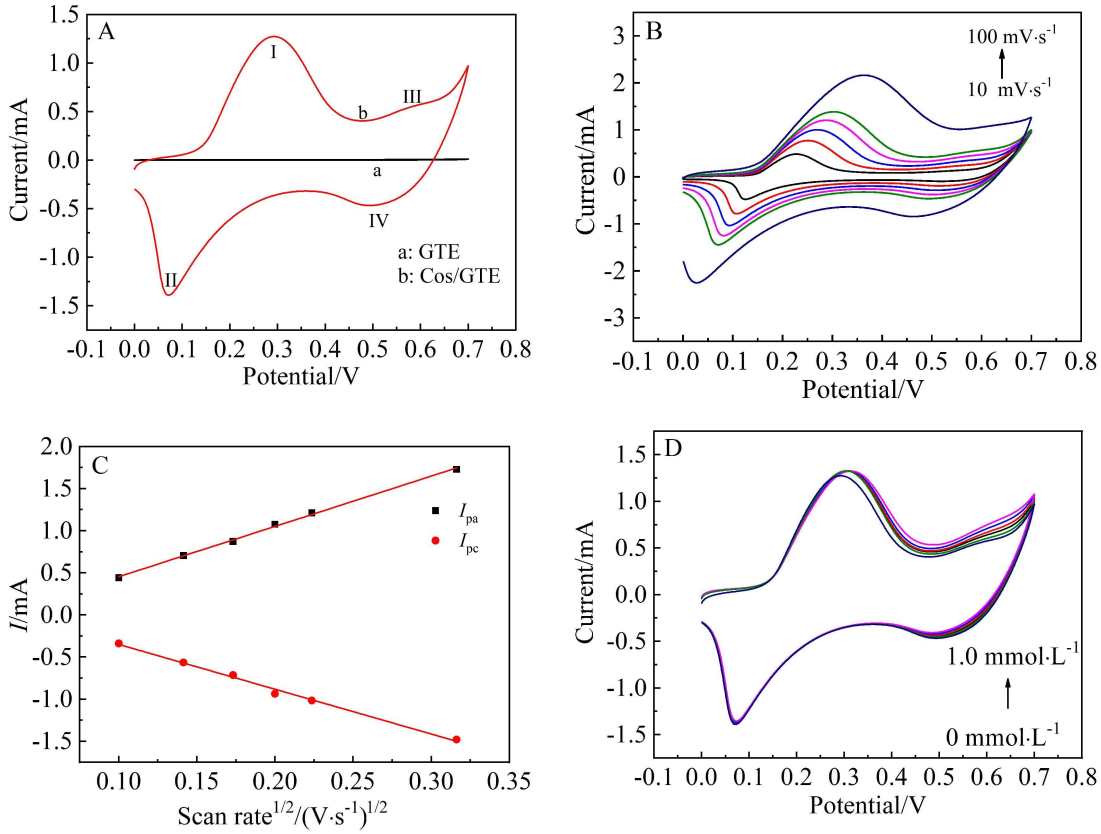

Figure 3 (A) CVs of bare GTE and CoS/GTE in 0.1 mol·L^{-1} NaOH (scan rate: 50 mV·s^{-1}). (B) CVs of CoS/GTE in 0.1 mol·L^{-1} NaOH at different scan rates from 10 to 100 mV·s^{-1}. (C) The Plots of cathodic and anodic peak currents vs. square root of scan rate. (D) CVs of CoS/GTE from 0 to 1.0 mmol·L^{-1} glucose in 0.1 mol·L^{-1} NaOH (scan rate: 50 mV·s^{-1}). (color on line)

accelerate the transformation of glucose into gluconolactone, which is widely accepted that the oxidation reaction is through 2-electron electrochemical reaction[41]. Meanwhile, it can be seen that the current connected with the Co^{2+}/Co^{3+} redox couple remained nearly unchanged with increasing the concentration of glucose, while the increase of the anodic peak current connected with the oxidation of Co^{3+} species was observed, manifesting that it is chiefly catalyzed for the electrooxidation of glucose by $CoOOH/CoO_2$ rather than $Co(OH)_2/CoOOH$, which is in line with the previous report[39], as following equation (3):

With consuming CoO_2 and producing CoOOH, the extent of Reaction (2) would greatly favor the forward reaction ($CoOOH \rightarrow CoO_2$), which results in the increase of oxidation peak III upon the addition of glucose.

Figure 4(A) displays the amperometric current responses of CoS/GTE with continuously adding 0.2 mmol·L^{-1} glucose at different applied potentials (0.45 V, 0.5 V, 0.55 V) in 0.1 mol·L^{-1} NaOH. An obvious current response was noticed with increasing the applied potential, however, upon applying 0.55 V, it caused a high background current. Therefore, 0.50 V was selected as the optimal potential for the following current measurement. The typic amperometric responses upon consecutive droppings of glucose on the proposed sensor is shown in Figure 4(B). With the increase of glucose concentration, the current decreased. It is ascribed that adsorption of glucose could obstruct the mass transfer that influenced the fresh glucose molecules closer to the electrode surface

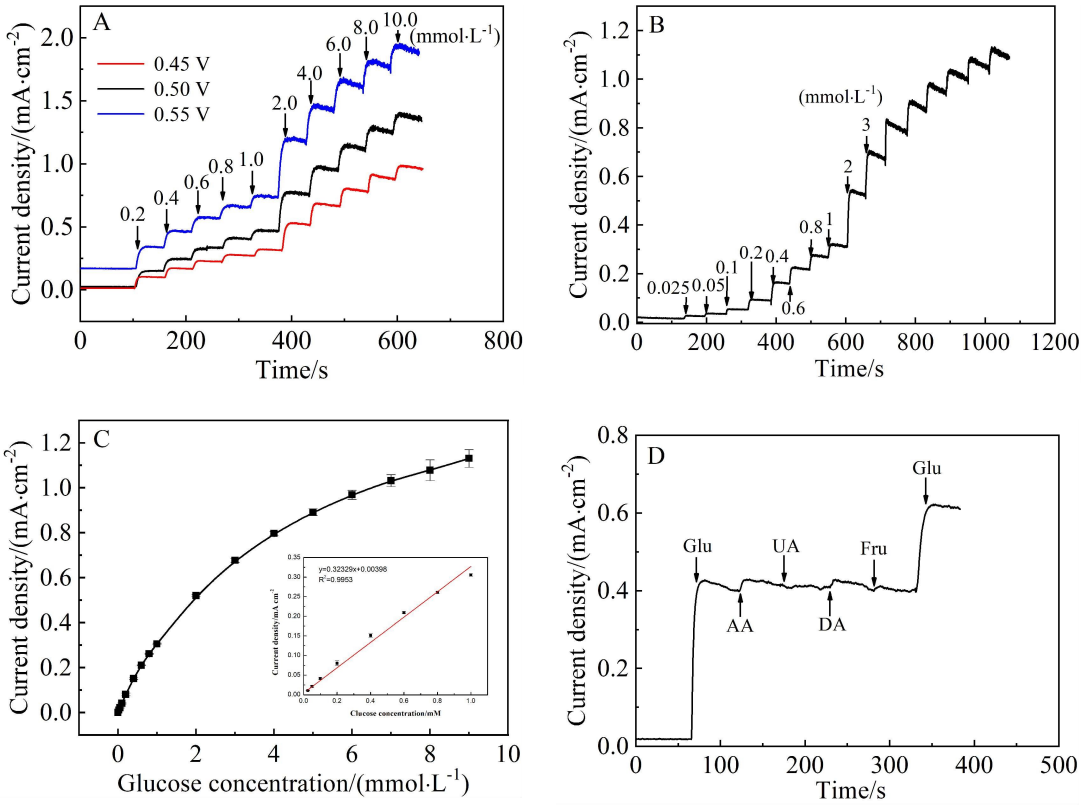

Figure 4 (A) Amperometric current responses of the CoS/GTE at different applied potentials (0.45, 0.50 V and 0.55 V) with different concentrations of glucose in 0.1 mol·L^{-1} NaOH. (B) Amperometric current responses of the CoS/GTE with successive addition of glucose in 0.1 mol·L^{-1} NaOH at 0.50 V. (C) The corresponding calibration curve for current responses to various glucose concentrations from 0.025 to 9.0 mmol·L^{-1} at 0.50 V. Inset shows the corresponding calibration curve established between response current and glucose concentration from 0.025 to 1.0 mmol·L^{-1}. (D) Amperometric current responses of the CoS/GTE against the addition of glucose (1.0 mmol·L^{-1}) and various co-existing interferents (0.1 mmol·L^{-1}, respectively) injected into in 0.1 mol·L^{-1} NaOH at 0.50 V. (color on line)

diffusing[20]. It can be seen that the corresponding calibration curve of the proposed sensor (Figure 4(C)) showed a linear response in the ranges of 0.025 ~ 1.0 mmol·L^{-1} (correlation coefficient R^2 = 0.9953), with a detection sensitivity of 323.29 μA·(mmol·L^{-1})$^{-1}$·cm^{-2} and a LOD of 8.5 μmol·L^{-1} (S/N = 3). Compared with the behaviors of other reported Co-based electrochemical nonenzymatic glucose sensors (Table 1), analytical parameters of our proposed sensor are satisfactory.

It is one of the indispensable concerns in the electrochemical glucose sensor to own good selectivity performance towards other physiological species including ascorbic acid (AA), dopamine (DA), uric acid (UA) and fructose (Fru). Therefore, the *I-t* curve was measured in order to investigate the influence of common interferents on glucose oxidation at a fixed potential. As shown in Figure 4(D), it can be evidently seen that the CoS/GTE had a notable response for glucose, the interference signals of AA and DA current responses to the glucose were 2.98% and 3.33%, respectively, while no apparent responses of UA and Fru to the glucose were presented. By add glucose, the current density increased again. Considering that the blood glucose level for a healthy person (3 ~ 8 mmol·L^{-1}) is prominently higher than that of the competing interferents, such as UA (0.33 mmol·L^{-1}) and AA (0.125 mmol·L^{-1})[40], it can be concluded that the CoS/GTE exhibited superior selectivity toward glucose detection, which can potentially applied in clinical analysis of in vitro glucose.

The repeatability of the CoS/GTE was tested. The consecutive tests were carried out at the same CoS/GTE in 0.1 mol·L^{-1} NaOH including 0.5 mmol·L^{-1} glucose for five parallel times. The calculated RSD of the glucose oxidation-current response for each measurement was 3.38%, demonstrating a good repeatability of the fabricated CoS/GTE.

For reproducibility assessment, five as-obtained CoS/GTEs sensors were examined under the same

Table 1 Comparison of analytical performances for different Co-based sensors.

Electrode material	Method	Sensitivity (μA·cm^{-2}·(mmol·L^{-1})$^{-1}$)	Linear range/ (mmol·L^{-1})	Test Potential/V	Detection Limit/ (μmol·L^{-1})	Flexible substrate	Ref.
CoS	Hydrothermal method	139.35; 28.44	0.005 ~ 1.10; 1.20 ~ 10.20	0.20	1.5	No	[20]
CoS/3D porous carbon skeleton	Hydrothermal method	679	0.01 ~ 0.9	0.45	2	No	[21]
Co_xS_y/ rGO-PEDOT	CV	113.46	0.0002 ~ 1.380	0.65	0.079	No	[22]
Nickel-cobalt phosphate	Hydrothermal method	302.99	0.002 ~ 4.47	0.55	0.4	No	[42]
$NiCo_2S_4$/Ni/CFP	CV	283	0.0005 ~ 6	0.45	0.05	Yes	[43]
3D graphene frameworks/ Co_3O_4 composites	Sol-gel	122.16	0.025 ~ 0.080	0.58	0.157	No	[44]
CoTsPc	-	122.5	0.01 ~ 6.34	–	0.14	No	[45]
CoOOH nanosheets	Redox reaction	341	0.03 ~ 0.7	0.4	30.9	No	[46]
CoP	Precipitation method	116.8	0.5 ~ 5.5		9	No	[47]
CoS/GTE	CA	323.3	0.025 ~ 1.0	0.5	8.5	Yes	This work

Table 2 Results for detection of glucose in human serum samples (n = 3)

Spiked/ (μmol·L^{-1})	Detected/ (μmol·L^{-1})	RSD/%	Mean recovery/%
25	25.63	3.92	102.5
50	48.25	4.84	96.5
75	72.55	4.51	96.7

conditions using 0.5 mmol·L^{-1} glucose in 0.1 mol·L^{-1} NaOH. The RSDs were calculated to be 6.03%, evincing a good reproducibility. After being stored in air exposure for half a month, the CoS/GTE showed 85.7% of its initial response current, indicating that the enzymeless CoS/GTE glucose sensor owns agreeable stability[12].

3.4 Practical Applications

To validate the applicability of the CoS/GTE, the detection of the glucose in healthy human blood serum sample was further investigated with the glucose concentration of 5.20 mmol·L^{-1} by the standard addition method. The original serum sample was diluted using 0.1 mol·L^{-1} NaOH, and then the given concentration of glucose was drop by drop added into the serum sample. It indicates an acceptable recovery ranging from 96.5 to 102.5% in human serum samples with RSD from 3.92% ~ 4.84%(Table 1). Hence, the CoS/GTE can be used as a potential sensor for the determining glucose in human serum samples.

4 Conclusions

The flexible, binderless and self-supporting CoS/GTE fabricated by electrodeposition was directly employed as an efficient nonenzymatic glucose sensor. The sensor exhibited high sensitivity which might be attributed to the high reaction surface area and ample electroactive sites of flower-like CoS, and good electron transfer ability of GTE. Its application for glucose analysis in human serum was also demonstrated successfully. The results indicate that CoS/GTE is a promising contestant for enzymeless glucose sensor. Meanwhile, the proposed sensor offers a very promising electrode material toward many further electrochemical applications with its flexibility, disposability, portability and low price.

Acknowledgements:

This work was financially supported by Applied Basic Research Program of Datong (No. 2018147), Natural Science Foundation of Shanxi Province (No. 201801D121035), Natural Science Foundation of Datong (No. 201819), Scientific and Technological Innovation Programs of Higher Education Institutions in Shanxi (No. 2019L0735, No. 2020L0478, No. 2020L0498), Cultivate Scientific Research Excellence Programs of Higher Education Institutions in Shanxi (No. 2020KJ023), Key Scientific and Technological Projects of Datong City (No. 2018014) as well as the Special Key Laboratory of Guizhou Province (No. [2018]004), the Science Foundation of the Science and Technology Department of Guizhou Province (No. [2014]17), and Natural Science Research Project of the Education Department of Guizhou Province (No. [2015]386), Science and Technology of Sichuan Province (No. 2016JY0096).

References:

[1] Rahman M M, Ahammad A J S, Jin J H, Ahn S J, Lee J J. A comprehensive review of glucose biosensors based on nanostructured metal-oxides[J]. Sensors, 2010, 10(5): 4855-4866.

[2] Desmet C, Marquette C A, Blum L J, Doumèche B. Paper electrodes for bioelectrochemistry: Biosensors and biofuel cells[J]. Biosens. Bioelectron. 2016, 76(SI): 145-163.

[3] Gabriel E F M, Garcia P T, Cardoso T M G, Lopes F M, Martins F T, Coltro W K T. Highly sensitive colorimetric detection of glucose and uric acid in biological fluids using chitosan-modified paper microfluidic devices[J]. Analyst, 2016,141(15): 4749-4756.

[4] Hwang D W, Lee S, Seo M, Chung T D. Recent advances in electrochemical non-enzymatic glucose sensors - a review[J]. Anal. Chim. Acta, 2018, 1033: 1-34.

[5] Qiu H W, Xu S C, Jiang S Z, Li Z, Chen P X, Gao S S, Zhang C, Feng D J. A novel graphene-based tapered optical fiber sensor for glucose detection[J]. Appl. Surf. Sci., 2015, 329: 390-395.

[6] Nicholas D, Logan K A, Sheng Y J, Gao J H, Farrell S, Dixon D, Callan B, McHale A P, Callan J F. Rapid paper based colorimetric detection of glucose using a hollow

microneedle device[J]. Int. J. Pharm., 2018, 547(1-2): 244-249.

[7] Shoji A, Takahashi Y, Osato S, Sugawara M. An enzyme-modified capillary as a platform for simultaneous fluorometric detection of D-glucose and L-lactate[J]. Pharm. Biomed. Anal., 2019, 163: 1-8.

[8] Zhu C Z, Yang G H, Li H, Du D, Lin Y H. Electrochemical sensors and biosensors based on nanomaterials and nanostructures[J]. Anal. Chem., 2015, 87(1): 230-249.

[9] Mohamad N R, Marzuki N H C, Buang N A, Huyop F, Wahab R A. An overview of technologies for immobilization of enzymes and surface analysis techniques for immobilized enzymes[J]. Biotechnol. Biotechnol. Equip., 2015, 29(2): 205-220.

[10] Yu Y Y, Yang Y, Gu H, Zhou T S, Shi G Y. Size-tunable Pt nanoparticles assembled on functionalized ordered mesoporous carbon for the simultaneous and on-line detection of glucose and L-lactate in brain microdialysate [J]. Biosens. Bioelectron., 2013, 41: 511-518.

[11] Ye J S, Chen C W, Lee C L. Pd nanocube as non-enzymatic glucose sensor[J]. Sensor Actuat. B - Chem., 2015, 208: 569-574.

[12] Malhotra S, Tang Y J, Varshney P K. Non-enzymatic glucose sensor based on electrodeposition of platinum particles on polyaniline modified Pt electrode[J]. Anal. Bioanal. Electrochem., 2018, 10(6): 699-715.

[13] Wang R L, Liang X Y, Liu H Y, Cui L, Zhang X Y, Liu C J. Non-enzymatic electrochemical glucose sensor based on monodispersed stone-like PtNi alloy nanoparticles[J]. Microchim. Acta, 2018, 185(7): 339.

[14] Shim K, Lee W C, Park M S, Shahabuddin M, Yamauchi Y, Hossain M S A, Shim Y B, Kim J H. Au decorated core-shell structured Au@ Pt for the glucose oxidation reaction[J]. Sensor Actuat. B - Chem., 2019, 278: 88-96.

[15] Yang J W, Liang X Y, Cui L, Liu H Y, Xie J B, Liu W X. A novel non-enzymatic glucose sensor based on Pt3Ru1 alloy nanoparticles with high density of surface defects [J]. Biosens. Bioelectron., 2016, 80: 171-174.

[16] Sheng Q, Mei H, Wu H M, Zhang X H, Wang S F. A highly sensitive non-enzymatic glucose sensor based on Pt_xCo_{1-x}/C nanostructured composites[J]. Sensor Actuat. B - Chem., 2015, 207: 51-58.

[17] Koskun Y, Savk A, Sen B, Sen F. Highly sensitive glucose sensor based on monodisperse palladium nickel/activated carbon nanocomposites[J]. Anal. Chim. Acta, 2018, 1010: 37-43.

[18] Lai C H, Lu M Y, Chen L J. Metal sulfide nanostructures: synthesis, properties and applications in energy conversion and storage[J]. Mater. Chem., 2012, 22(1): 19-30.

[19] Wang J H, Cui W, Liu Q, Xing Z C, Asiri A M, Sun X P. Recent progress in cobalt-based heterogeneous catalysts for electrochemical water splitting[J]. Adv. Mater., 2016, 28(2): 215-230.

[20] Wu W Q, Yu B B, Wu H M, Wang S F, Xia Q H, Ding Y. Synthesis of tremella-like CoS and its application in sensing of hydrogen peroxide and glucose[J]. Mater. Sci. Eng. C, 2017, 70: 430-443.

[21] Qu P P, Gong Z N, Cheng H Y, Xiong W, Wu X, Pei P, Zhao R F, Zeng Y, Zhu Z H. Nanoflower-like CoS-decorated 3D porous carbon skeleton derived from rose for a high performance nonenzymatic glucose sensor[J]. RSC Adv., 2015, 5(129): 106661-106667.

[22] Meng A, Sheng L Y, Zhao K, Li Z J. A controllable honeycomb-like amorphous cobalt sulfide architecture directly grown on the reduced graphene oxide-poly (3,4-ethylenedioxythiophene) composite through electrodeposition for non-enzyme glucose sensing[J]. Mater. Chem. B, 2017, 5(45): 8934-8943.

[23] Sivakumar M, Sakthivel M, Chen S M. Simple synthesis of cobalt sulfide nanorods for efficient electrocatalytic oxidation of vanillin in food samples[J]. J. Colloid Interface Sci., 2017, 490: 719-726.

[24] Kang Z, Li Y, Cao S Y, Zhang Z H, Guo H J, Wu P W, Zhou L X, Zhang S C, Zhang X M, Zhang Y. 3D graphene foam/ZnO nanorods array mixed-dimensional heterostructure for photoelectrochemical biosensing[J]. Inorg. Chem. Front., 2018, 5(2): 364-369.

[25] Niu J A, Domenech-Carbo A, Primoa A, Garcia H. Uniform nanoporous graphene sponge from natural polysaccharides as a metal-free electrocatalyst for hydrogen generation[J]. RSC Adv., 2019, 9(1): 99-106.

[26] Han W J, Ren L, Gong L J, Qi X, Liu Y D, Yang L W, Wei X L, Zhong J X. Self-assembled three-dimensional graphene-based aerogel with embedded multifarious functional nanoparticles and its excellent photoelectrochemical activities[J]. ACS Sustainable Chem. Eng., 2014, 2(4): 741-748.

[27] Chen D M, Yang J J, Zhu Y, Zhang Y M, Zhu Y F. Fabrication of BiOI/graphene Hydrogel/FTO photoelectrode with 3D porous architecture for the enhanced photoelectrocatalytic performance[J]. Appl. Catal. B - Environ., 2018, 233: 202-212.

[28] Chen D, Zhang H, Liu Y, Li J H. Graphene and its derivatives for the development of solar cells, photoelectrochemical, and photocatalytic applications[J]. Energy Environ. Sci., 2013, 6(5): 1362-1387.

[29] Baig N, Saleh T A. Electrodes modified with 3D graphene composites: a review on methods for preparation, proper-

ties and sensing applications[J]. Microchim. Acta, 2018, 185(6): 283.

[30] Ito Y, Tanabe Y, Sugawara K, Koshino M, Takahashi T, Tanigaki K., Aokighi H, Chen M W. Three-dimensional porous graphene networks expand graphene-based electronic device applications[J]. Phys. Chem. Chem. Phys., 2018, 20(9): 6024-6033.

[31] Wang L, Yu J, Zhang Y Y, Yang H, Miao L F, Song Y H. Simple and large-scale strategy to prepare flexible graphene tape electrode[J]. ACS Appl. Mater. Interfaces, 2017, 9(10): 9089-9095.

[32] Lange B, Lovric M, Scholz F. The catalytic action of ad sorbed thiocyanate ions and thiourea in the electron transfer from glassy carbon to solid copper(I) selenide and copper(I) sulfide particles[J]. Electroanal. Chem., 1996, 418(1-2): 21-28.

[33] Nan K K, Du H F, Su L, Li C M. Directly electrodeposited cobalt sulfide nanosheets as advanced catalyst for oxygen evolution reaction[J]. ChemistrySelect, 2018, 3(25): 7081-7088.

[34] Gao R, Liu L, Hu Z B, Zhang P, Cao X Z, Wang B Y, Liu X F. The role of oxygen vacancies in improving the performance of CoO as a bifunctional cathode catalyst for rechargeable Li-O_2 batteries[J]. Mater. Chem. A, 2015, 3 (34): 17598-17605.

[35] Mao M L, Jiang L, Wu L C, Zhang M, Wang T H. The structure control of ZnS/graphene composites and their excellent properties for lithium-ion batteries[J]. Mater. Chem. A, 2015, 3(25): 13384-13389.

[36] Shi J H, Li X C, He G H, Zhang L, Li M. Electrodeposition of high-capacitance 3D CoS/graphene nanosheets on nickel foam for high-performance aqueous asymmetric supercapacitors[J]. Mater. Chem. A, 2015, 3(41): 20619-20626.

[37] Bahadur S, Gong D L. The investigation of the action of fillers by XPS studies of the transfer films of PEEK and its composites containing CuS and CuF_2[J]. Wear, 1993, 160(1): 131-138.

[38] Huang K J, Zhang J Z, Shi G W, Liu Y M. One-step hydrothermal synthesis of two-dimensional cobalt sulfide for high-performance supercapacitors[J]. Mater. Lett., 2014, 131: 45-48.

[39] Liu Y W, Cao X Q, Kong R M, Du G, Asiri A M, Lu Q, Sun X P. Cobalt phosphide nanowire array as an effective electrocatalyst for non-enzymatic glucose sensing[J]. Mater. Chem. B, 2017, 5: 1901-1904.

[40] Chakrabartty S, Karmakar S, Raj C R. An electrocatalytically active nanoflake-like Co_9S_8-$CoSe_2$ het erostructure for overall water splitting[J]. ACS Appl. Nano Mater., 2020, 3(11): 11326-11334.

[41] Park S, Boo H, Chung T D. Electrochemical non-enzymatic glucose sensors[J]. Anal. Chim. Acta, 2006, 556(1): 46-57.

[42] Shu Y, Li B, Chen J Y, Xu Q, Pang H, Hu X Y. Facile synthesis of ultrathin nickel-cobalt phosphate 2D nanosheets with enhanced electrocatalytic activity for glucose oxidation[J]. ACS Appl. Mater. Interfaces, 2018, 10(3): 2360-2367.

[43] Babu K J, Kumar T R, Yoo D J, Phang S M, Kumar G G. Electrodeposited nickel cobalt sulfide flowerlike architectures on disposable cellulose filter paper for enzyme-free glucose sensor applications[J]. ACS Sustainable Chem. Eng., 2018, 6(12): 16982-16989.

[44] Bao L, Li T, Chen S, Peng C, Li L, Xu Q, Chen Y S, Ou E C, Xu W J. 3D graphene frameworks/Co_3O_4 composites electrode for high-performance supercapacitor and enzymeless glucose detection[J]. Small, 2017, 13(5): 1602077.

[45] Devasenathipathy R, Karuppiah C, Chen S M, Palanisamy S, Lou B S, Ali M A, Al-Hemaid F M A. A sensitive and selective enzyme-free amperometric glucose biosensor using a composite from multi-walled carbon nanotubes and cobalt phthalocyanine[J]. RSC Adv., 2015, 5(34): 26762-26768.

[46] Lee K K, Loh P Y, Sow C H, Chin W S. CoOOH nanosheets on cobalt substrate as a non-enzymatic glucose sensor[J]. Electrochem. Comm., 2012, 20: 128-132.

[47] Sun Q Q, Wang M, Bao S J, Wang Y C, Gu S. Analysis of cobalt phosphide (CoP) nanorods designed for non-enzyme glucose detection[J]. Analyst, 2016, 141(1): 256-260.

一种基于电沉积 3D 花状 CoS 在自支撑石墨烯胶带电极上的非酶葡萄糖传感器的研究与应用

李 江[1], 李作鹏[1], 白云峰[1], 罗宿星[2], 郭 永[1],
鲍雅妍[1], 李 容[3], 刘海燕[4], 冯 锋[1*]

(1. 山西大同大学化学与化工学院,山西 大同 037009;2. 遵义师范学院,贵州 遵义 563006;
3. 西华师范大学化学化工学院,四川 南充 637000;4. 山西大同大学生命科学院,山西 大同 037009)

摘要: 本文将 3D 纳米结构花状 CoS 电沉积在石墨烯胶带电极(GTE)上,制备了一种对葡萄糖响应良好的电化学传感器。结构分析显示电沉积的 CoS 均匀地分散在了电极上。实验结果表明,制备的花状 CoS/GTE 葡萄糖传感器在 0.025 ~ 1.0 mmol·L^{-1} 显示出良好的线性关系,灵敏度为 323.3 μA·(mmol·L^{-1})$^{-1}$·cm^{-2},检出限为 8.5 μmol·L^{-1} (S/N = 3),而且制备的传感器能够应用于血清葡萄糖的检测。这表明本文制备的传感器具有一定的应用潜力。

关键词: 柔性电极;花状 CoS;电沉积;葡萄糖传感器